Water and halogens in volcanic clasts: tracers of degassing processes during Plinian and dome-building eruptions

B. VILLEMANT[1], G. BOUDON[1,2], S. NOUGRIGAT[1], S. POTEAUX[1] & A. MICHEL[1]

[1]*Physique et Chimie des Systèmes volcaniques, Institut de Physique du Globe de Paris, Université Pierre et Marie Curie and CNRS-UMR 7046 (Géomatériaux), Boîte 109, 4 place Jussieu, 75005 Paris, France.*
(e-mail: villemant@ipgp.jussieu.fr)
[2]*Observatoires Volcanologiques, IPGP, Boîte 89, 4 place Jussieu, 75005 Paris, France.*

Abstract: Magma degassing may occur either with no significant gas escape from the magma column, which corresponds with typical Plinian type eruptions, or with gas loss, which corresponds with typical effusive (dome-building) eruptions. Magma degassing may also lead to melt crystallization, which modifies the residual melt composition and, in turn, may significantly affect the degassing conditions. We propose a method for modelling these processes for H_2O-rich rhyolitic melts through measurements of volatiles (H_2O, Cl, Br) in the microcrystalline matrix and glass of erupted volcanic clasts (pumice and dome clasts). This method is applied to two Plinian and dome-building eruptions at Mount Pelée (Martinique) and Santa Maria (Guatemala) volcanoes. Extreme magma degassing and crystallization during dome-building eruptions may explain the contrasts in halogen and H_2O contents of residual melts of dense volcanic clasts: they display very large ranges of Cl contents (few ppm to thousands of ppm), whereas the ranges of H_2O contents are much narrower, and lower than 1%. This method allows prediction of the evolution of volcanic gas chemistry (as HCl content or HCl/HF ratio) as a function of the degassing style of magma at shallow depth.

Eruptive styles of H_2O-rich silicic magmas vary from effusive to highly explosive. Water degassing at shallow depths constitutes the main source of energy in these eruptions, and the eruptive styles are controlled by the evolution of the fluid phase during magma ascent (exsolution, bubble expansion, and gas loss) and the bulk magma rheology (density and viscosity), which are interdependent (Eichelberger *et al.* 1986; Eichelberger 1995, Jaupart & Allègre 1995; Sparks 1997; Melnik & Sparks 1999; Sparks 2003). In particular, microlite crystallization related to melt degassing may play an important role by increasing melt crystallinity and hence bulk magma viscosity (Lejeune & Richet 1995).

The syn-eruptive evolution of the aqueous fluid phase in magmas is complex and depends on many parameters, such as solubility, diffusivity, and expansion, which are controlled by pressure, temperature, melt composition (particularly the initial fluid content), rate of fluid escape from the magma column (through the wall-rocks or due to differential movement between the gas phase and the magma), and degassing-related microlite crystallization. Based on simple thermo- and hydro-dynamic considerations, it is possible to establish theoretical models that, for different eruptive styles, describe the theoretical evolution of the exsolved and residual fluids (Jaupart & Allegre 1991; Sparks 1997; Villemant & Boudon 1998; Melnik & Sparks 1999). However, applications to real eruptions remain difficult because the determination of the compositions of the exsolved fluids (volcanic gases), or of the fluids dissolved in erupted products, is technically complex and may involve large measurement uncertainties, especially for major components such as H_2O (see e.g. Ihinger *et al.* 1994; Symonds *et al.* 1994). The use of halogens to follow degassing processes is of interest because their behaviour is mainly controlled by their partitioning into the H_2O-rich fluid phase, and the analysis of these elements in natural systems (glasses, melt inclusions, and volcanic gases) is generally easier and more accurate than for H_2O. Thus, measurement of halogen contents of primary melt inclusions and in erupted magmas (pumice or dome clasts) allows reconstruction of

From: OPPENHEIMER, C., PYLE, D.M. & BARCLAY, J. (eds) *Volcanic Degassing*. Geological Society, London, Special Publications, **213**, 63–79. 0305–8719/03/$15.00

the bulk H_2O degassing path during an eruptive event (Villemant & Boudon 1998, 1999). Moreover, the evolution of the bulk gas phase composition may be deduced from these models and compared with compositions of volcanic gas plumes (Villemant & Boudon 1999, Edmonds *et al.* 2001).

Here we present a refinement of the model proposed by Villemant & Boudon (1999) to describe shallow-depth degassing of H_2O-rich silicic melts subject to decompression and crystallization. The model gives consistent interpretations of residual H_2O and halogen contents of magmatic clasts erupted during Plinian and dome-building (effusive) eruptions from different active volcanoes: Mount Pelée (Martinique, Lesser Antilles: 650 years BP eruption) and Santa Maria-Santiaguito (Guatemala: Plinian and dome-building eruptions since 1902).

Modelling degassing processes

Major volatile species (mainly H_2O in the silicic magmas of interest) dissolved in melts may reach saturation in response to a pressure decrease or to variations of the melt composition, due, for example, to crystallization. Then a fluid phase exsolves and the magma vesiculates, decreasing the bulk magma density. If the magma is able to rise, the pressure decrease induces both an expansion of the bubbles and a decrease of the volatile solubility in the melt. In addition, the melt may also crystallize in response to gas loss, increasing, in turn, the volatile content in the residual melt, and hence promoting the degassing process.

Closed- and open-system evolution

If the system remains closed (i.e. there is no significant differential motion between melt and gas phase), bubble expansion and increase of the mass fraction of the exsolved fluid phase lead to an increase in the magma ascent velocity. When the magma contains a large volume fraction of bubbles (60–75%) it can fragment: i.e. the magma, which constitutes a continuous medium containing melt, crystals, and gas bubbles, is transformed into a continuous gas medium containing vesiculated magmatic clasts (pumice). The gas jet then evolves differently in response to an extremely rapid gas expansion (Wilson *et al.* 1980). This model corresponds with an ideal Plinian type eruption. It is generally assumed that, at fragmentation, the melt is quenched, and no further significant volatile exsolution occurs. Moreover, in this model, since eruption rates are high, it is assumed that the melt composition remains constant over the whole degassing path (in particular, no microlite crystallization occurs). This is consistent with the common observation that pumice glass is generally homogeneous and lacking in microlites. Thus, between H_2O-saturation and fragmentation, the degassing history of a H_2O-rich magma may be described using the well-known solubility law of H_2O in melts and the perfect gas law (gas expansion), if equilibrium is assumed between the melt and the exsolved gas phase (Burnham 1979, 1994; Jaupart & Allègre 1991; Villemant & Boudon 1999).

For open-system evolution models, it is assumed, in addition, that the exsolved gas fraction has had time to escape from the source magma, either through wall-rocks by percolation, or through the volcanic vent itself by differential motion between the more rapidly ascending gas phase and the magma. In this case, eruption rates are much lower than in closed-system evolution. This corresponds with effusive (dome-building) type eruptions. In such cases, H_2O escape may induce melt crystallization (Burnham 1979; Swanson *et al.* 1989; Cashman 1992; Hammer *et al.* 1999). In addition, if gas escapes from the permeable magma by bubble connection (the permeable foam model of Eichelberger *et al.* 1986), the internal gas pressure of these bubbles is no longer maintained, and the bubbles collapse. Highly microlitic groundmass, irregular and flattened vesicles, and low residual gas contents are common features of lava-dome magmas. In models, these processes are taken into account by adding Rayleigh distillation equations for both gas loss and melt crystallization to the closed-system equations (Villemant & Boudon 1998, 1999; Melnik & Sparks 1999). In addition, a relationship between bubble collapse rate and parameters such as decompression rate or magma crystallinity is needed for describing the evolution of the magma vesicularity (Villemant *et al.* 1996).

Erupted magmatic clasts: samples from different degassing steps

It has been shown (Bursik 1993; Gardner *et al.* 1996; Villemant & Boudon 1998) that different magmatic clasts emitted during the same eruptive stage may have followed different degassing histories in the magma conduit. Thus, during a typical Plinian eruption, erupting products mainly consist of vesiculated clasts with glassy matrix (pumice) characteristic of a closed-system evolution, but they may also contain more crystallized and degassed magma fragments corresponding with the evolution of degassing in an open system with significant melt crystallization (Hammer *et al.* 1998; Villemant & Boudon 1998; Blundy & Cashman 2001, among others). Similarly, open-system, effusive dome-building eruptions generally give rise to a highly degassed and microcrystalline matrix, but also to degassed, glassy and unvesiculated obsidians or to less degassed, glassy and highly vesiculated clasts. More rarely, these eruptions are interrupted by short 'Vulcanian' episodes, as on 9 July 1902 at Mount Pelée, Martinique (Bourdier *et al.* 1989), or on 17 September 1996 and August–September 1997 at Soufrière Hills, Montserrat (Robertson *et al.* 1998). Thus, measurement of residual volatile contents in glasses from a large sample of erupted products in the same eruptive unit gives a more or less complete record of the degassing paths characteristic of the eruption dynamics.

Halogens in glasses: a tool for modelling degassing processes

The behaviour of minor volatile species extracted from the melt by the H_2O vapour may be simply deduced from the preceding degassing models by using partition coefficients between vapour and melt. Halogens display a wide spectrum of distribution coefficients between H_2O-rich fluids and melts (d^i_{v-l}). Experimental determinations of halogen partitioning show that d^i_{v-l} values strongly increase from *F* to *I* ($d^F_{v-l} < 1 << d^{Cl}_{v-l} < d^{Br}_{v-l} << d^I_{v-l}$; Kilinc & Burnham 1972; Webster & Holloway 1988; Shinohara *et al.* 1989; Métrich & Rutherford 1992; Webster 1992; Bureau *et al.* 2000). These results have been confirmed by modelling F, Cl, and Br behaviour in Plinian eruptions (Villemant & Boudon 1999). Since halogens are highly incompatible elements in magmas, degassing-related melt crystallization induces an increase of their concentration in residual melts which may be simply calculated from the crystallization rate. Degassing-induced crystallization and gas escape have opposite effects on H_2O and halogen contents in the melt, and the net effect is directly dependent on the ratio between crystallization and degassing rates. In addition, experimental studies show that vapour–melt partioning of halogens is also strongly dependent on the melt composition (Shinohara *et al.* 1989; Webster 1992; Signorelli & Carroll 2000, 2001, and discussion below).

Concentrations of halogens in initial and residual melts may be measured by different techniques with accuracies generally better than for H_2O: *in situ* measurements for F and Cl by electron- or ion-probe (residual glasses and melt inclusions) and bulk-rock measurements of F, Cl, and Br by pyrohydrolysis extraction and ion chromatography or ICP–MS (Ihinger *et al.* 1994; Schnetger *et al.* 1998). The H_2O and halogen content of the bulk groundmass (residual melt+microlites) may be simply calculated from bulk rock sample measurements, by correcting for phenocryst contents (see Villemant & Boudon 1998 and below).

Equations for open- and closed-system evolution

The following is a revised and extended formulation of equations given by Villemant & Boudon (1999). The isothermal degassing evolution for H_2O and a minor volatile species (1) characterized by its vapour–melt partition coefficient (d^i_{v-l}) are described by the following two equations:

$$X_{H_2O}=S_{H_2O}\,P^{n}{}_{H_2O} \quad (1)$$

(H_2O solubility law)

$$d^i_{v-l}=(x_i^0/x_i-1)/(X^0_{H_2O}-X_{H_2O}) \quad (2)$$

where S_{H_2O} and n_{H_2O} are constants and *P* is the pressure. $X^0_{H_2O}$ and x_i^0 are the initial melt contents (i.e. at saturation pressure) of H_2O and element *i*, and X_{H_2O} and x_i the corresponding residual melt contents at pressure *P*. Typical values for these parameters in rhyolitic melts are given in Table 1. Initial melt compositions

Table 1. *Thermochemical characteristics of the reference rhyolitic melt.*

Rhyolitic melt	T	S_{H_2O}*	n_{H_2O}	K_R*	Initial melt†	H_2O	F	Cl	Br
	900 °C	0.321	0.54	14	d^i_{v-l}	–	<0.1	20	18
					X^i_0	5.5%	270 ppm	2100 ppm	6.2 ppm

S_{H_2O} and n_{H_2O} values are from Villemant & Boudon (1998).
*If *P* is expressed in MPa and X_{H_2O} in %.
†Initial melt composition of the 650 years BP eruption at Mount Pelée (Villemant & Boudon 1998; Martel *et al.* 1999).

($X^0_{H_2O}$, x_i^0) may be estimated from melt inclusions or experimental determination and d^i_{v-l} values from experimental determinations or degassing models. The $X^0_{H_2O}$ and x_i values are measured in residual glasses from erupted magmas.

Closed-system evolution

In this degassing model, the exsolved gas fraction remains confined in the magma, and the evolution of the volume of gas in bubbles is also controlled by the perfect gas law:

$$V_g/V_l = K_R\,(X^0_{H_2O} - X_{H_2O})/P \qquad (3)$$

where V_g/V_l is the ratio between the volumes of gas and melt at pressure P, and K_R is a constant (Table 1).

Open-system evolution

This degassing model assumes that the volatile phase escapes the reference melt volume after exsolution. The composition of the residual melt remains controlled by the H_2O solubility law, and the evolution of minor species may be described using a Rayleigh distillation law, which substitutes into equation (2) (Villemant & Boudon 1999).

If there is no melt crystallization, then the model may be expressed by the following set of equations:

$$x_i = x_i^0 f_v^{\delta i} \text{ with } \delta i = d^i_{v-l} - 1 \qquad (2b)$$

$$f_v = 1 - (X^0_{H_2O} - X_{H_2O}) \qquad (2c)$$

where $1 - f_v$ represents the fraction of exsolved fluid.

If melt crystallization also occurs, then we can write:

$$dm_L = -\,dm_V - dm_S$$

where m_L, m_V and m_S represent, respectively, the mass of melt, exsolving vapour, and crystallizing solid. It is assumed that crystallization and degassing are directly related (Burnham 1979, 1994; Villemant & Boudon 1998; Cashman & Blundy 2000); hence, we can write an additional equation:

$$dm_S = k_{SV}\,dm_V$$

If f_m represents the mass fraction of residual melt:

$$f_m = m_L/m^0_L = 1 - m_V/m^0_L\,(1 + k_{SV})$$
$$\approx 1 - (X^0_{H_2O} - X_{H_2O})\,(1 + k_{SV})$$

and $dm_L/m_L = df_m/f_m$

The system of equations describing the degassing–crystallization model is then:

$$dm_L = -\,dm_V\,(1 + k_{SV})$$

$$dx_i/x_i = (d^i_{v-l}/(1 + k_{SV}) - 1)\,dm_L/m_L$$

By integration and using the definition of f_m, this system of equations leads to:

$$x_i = x_i^0 f_m^{\Delta i} \text{ with } \Delta i = d^i_{v-l}/(1 + k_{SV}) - 1 \qquad (2d)$$

$$f_m \approx 1 - (X^0_{H_2O} - X_{H_2O})\,(1 + k_{SV}) \qquad (2e)$$

which substitute into equations (2b) and (2c).

Estimations of parameters

Estimation of k_{SV} values cannot be simply inferred from observations. The microlite mass fraction may be estimated on the basis of SEM or TEM measurements with, however, very large uncertainties and interpretation difficulties (see, for example, Cashman 1992). Direct estimates of vapour mass fraction in erupted clasts are impossible if gas loss occurs. However, for some simple melt compositions, phase diagrams in the presence of water are experimentally established. The well-known Q–Ab–Or diagram may be used as a good representation of rhyolitic melts (Tuttle & Bowen 1958; Cashman & Blundy 2000; Blundy & Cashman 2001). By direct measurements on phase diagrams or by using thermodynamic codes, the k_{SV} values may thus be calculated for different cases of interest. Simulations of isothermal decompression of rhyolitic melt, using either direct projections of melt compositions in the Q–Ab–Or diagram or MELTS code (Ghiorso & Sack 1995) – although not strictly valid for these compositions – show that the k_{SV} values vary quite widely over crystallization–decompression paths (5–40 or more, Nougrigat *et al.* in prep.). During isothermal decompression simulations, k_{SV} values are, to a first approximation, constant in steps with P decrease, and rise to higher values when new crystallizing phases (such as silica minerals) appear (Fig. 1). In addition, calculations show that for H_2O saturated rhyolitic melts, the k_{SV} values slightly increase with decreasing initial H_2O content.

Partition coefficients

These may be estimated using experimental data or by using the halogen–H_2O compositions of a

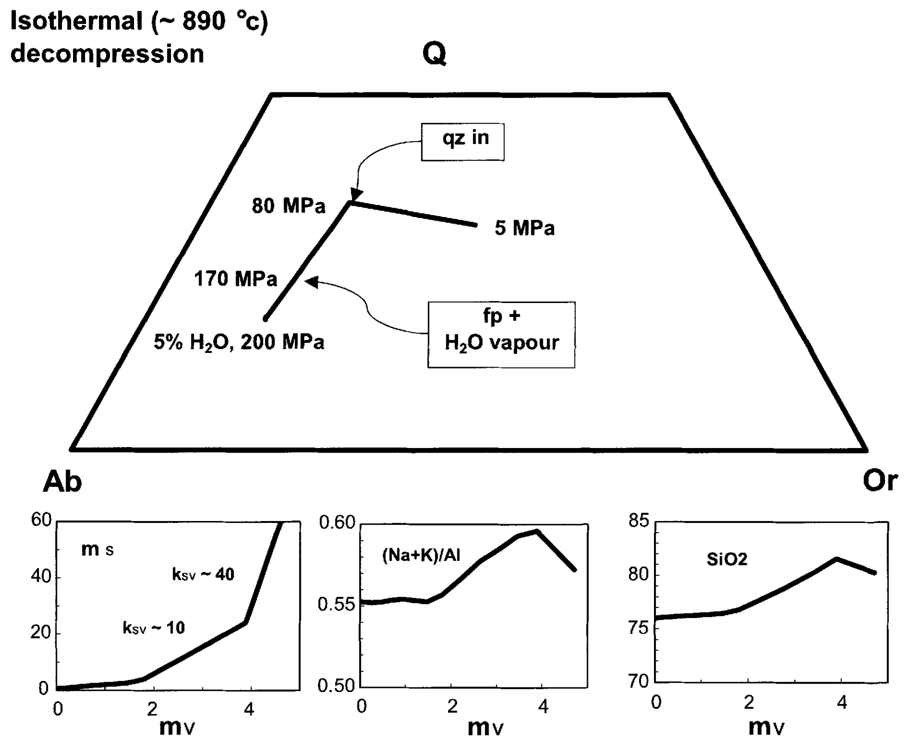

Fig. 1. Isothermal decompression of a H_2O-rich rhyolitic melt: the effects of shallow-depth decompression–crystallization on k_{SV}=dm_V/dm_S (m_V=mass of exsolving vapour and m_S=mass of crystallizing solid), SiO_2 content, and aluminous character of residual melts. The theoretical evolution of a natural rhyolitic melt (melt composition of the 650 years BP eruption at Mount Pelée) during isothermal (T *c.* 890 °C) degassing at low pressure (P <200 MPa) calculated using MELTS code (Ghiorso & Sack 1995) is represented in the Q–Ab–Or normative representation. The MELTS code is not established for rhyolitic compositions, and leads to some systematic bias. The comparison of MELT calculations on synthetic systems with experimental data allows correction of these biases, and shows that the relative variations of masses of melt, solid, and vapour formed at given conditions are not modified (Nougrigat *et al.* in preparation). Decompression path in the Q–Ab–Or diagram for a rhyolitic melt with an initial H_2O content of 5% H_2O. This melt is saturated relative to H_2O at *c.* 170 MPa, and crystallizes mainly Ab-rich plagioclase (fp). At low pressure (*c.* 80 MPa), a silica mineral phase joins plagioclase at the liquidus. The m_S–m_V diagram (the same arbitrary units are used on both axes) shows that the k_{SV} values (given by the slopes) are constant by steps. Crystallization of silica minerals leads to a strong increase in the k_{SV} value. The residual melt composition also strongly varies during degassing-induced crystallization, as shown by the evolution of the (Na+K)/Al ratio and SiO_2 content. The variations of the aluminous character and SiO_2 content of the residual melts may lead to large variations of the partition coefficients of volatile halogens between melt and vapour phase.

series of glasses that have degassed in a closed system (i.e. measured in clasts from Plinian eruptions; see Villemant & Boudon 1999). Experimental data show, however, that $d^{Cl}_{v\text{-}l}$ varies in a complex manner with T, P, and melt composition. The $d^{Cl}_{v\text{-}l}$ values increase with decreasing T and increasing P, if P >100–200 MPa, increasing SiO_2 and Cl contents of the melt (Webster 1992; Webster *et al.* 1999; Signorelli & Carroll 2000, 2001). The $d^{Cl}_{v\text{-}l}$ values vary strongly with the aluminous and peralkaline character of the melt, being maximum for (Na+K)/Al values close to 1 (Signorelli & Carroll 2001). For pressures below 100–200 MPa, because most experiments are using NaCl-bearing aqueous solutions, the fluids are in a subcritical condition, in which a NaCl brine and a Cl-poor aqueous fluid coexist. In this case, chlorine partitioning is affected by the phase relations in the fluid (Shinohara *et al.* 1989;

Signorelli & Carroll 2001). On the basis of the available experimental data at pressures <100–200 MPa, it is difficult to infer the actual d^{Cl}_{v-l} values and their dependence on pressure and composition. In addition, the experiments of Kravchuk and Keppler (1994) show that Cl partitioning between melt and H_2O vapour strongly differs in HCl-bearing and in NaCl- or KCl-bearing systems, suggesting that d^{Cl}_{v-l} values also strongly depend on the cation exchange (Na^+, K^+, or H^+) between vapour and melt. Since gaseous acids (HCl, HF, and HBr) are the dominant halogen-bearing species of juvenile magmatic gases, the results of Kravchuk and Keppler suggest that HCl-bearing experimental systems are more suitable than NaCl-bearing systems for measuring Cl partitioning during magma degassing at shallow depth, i.e. in conditions where metal-poor aqueous fluids are exsolved. In addition, some experiments suggest that kinetic effects may play an important role in halogen partitioning during shallow degassing processes (Gardner *et al.* 1998).

For rhyolitic melts at relatively high temperature (T >800 °C) and relatively low Cl contents (<2000 ppm), the available experimental data suggest that the main factors controlling d^{Cl}_{v-l} values are the SiO_2 content and the aluminous character of the residual melts. Calculations of residual melt composition in isothermal degassing experiments using the MELTS code show that (Na+K)/Al ratio and SiO_2 contents display significant variations: for the chosen example (Na+K)/Al ratio and SiO_2 content increase, respectively, from *c.*0.55 to *c.*0.60, and from *c.*75% to *c.*82% during plagioclase crystallization, and they decrease when silica minerals appear at the liquidus (Fig. 1). Larger ranges of (Na+K)/Al ratios (0.50–0.86) are displayed by residual melt compositions in dome fragments from eruptions at Mount Pelée and Santiaguito (Villemant & Boudon 1999, and S. Poteaux, unpublished data). As suggested by high-pressure (≥200 MPa) experiments, such variations should be able to induce significant increases of d^{Cl}_{v-l} values (typically from *c.*10–20 to values as high as *c.*50 or more; Webster 1992, Signorelli & Carroll 2001).

Vesicularity

In a closed-system evolution, the ratio V_g/V_l (3), which represents the magma vesicularity, may be estimated in erupted volcanic clasts by density measurements (Gardner *et al.* 1996; Villemant & Boudon 1999). However, in an open-system degassing model, gas loss is achieved either by differential motion of bubbles relative to melt or by the connection of bubbles (followed by flattening of the bubbles and their eventual complete disappearance). This excludes the possibility of establishing simple predictive models for the relationship between the final vesicularity and the residual volatile content of the melts: i.e. for open-system degassing, there is no straightforward equivalent to equation (3). In some cases, however, information on magma ascent rates may be obtained from the measured final vesicularity and the residual volatile contents of dome clasts, and assumptions of magma rheology (Villemant & Boudon 1998).

Correlation diagrams between residual volatile contents

The theoretical evolutions of residual melt compositions corresponding with the different models above are represented in H_2O–Cl, V_g/V_l–H_2O and V_g/V_l–Cl diagrams in Figure 2. For closed-system evolution, initial melt compositions and d^i_{v-l} values determined for the 650 years BP eruption at Mount Pelée have been used (Table 1). Arbitrarily, the open-system degassing processes are assumed to occur after a closed-system evolution step, from H_2O=2% in the residual melt.

Five sets of evolution curves are reported:

1. closed-system evolution from the initial melt composition (grey lines).
2. degassing without crystallization (dotted line).
3. degassing with crystallization, d^{Cl}_{v-l}=20, and k_{SV} varying between 10 and 40 (large open symbols).
4. the same as model (3), but assuming that d^{Cl}_{v-l} increases (20 to 40) in response to the variation of the residual melt composition (small open symbols)
5. same as model (4), but for Cl and H_2O contents of the bulk groundmass (residual glass+microlites; solid symbols).

Water–V_g/V_l diagrams may be used to distinguish closed-system and open-system evolution, as stated by Villemant & Boudon (1999), but they are not good at discriminating between the different open-system degassing models, regardless of which measurements are used (glass or bulk groundmass compositions). If only bulk groundmass compositions are used, it is seen that Cl–V_g/V_l or H_2O–V_g/V_l and Cl–H_2O diagrams cannot discriminate between the different degassing–crystallization models (solid symbols). In addition, if no crystallization occurs, the

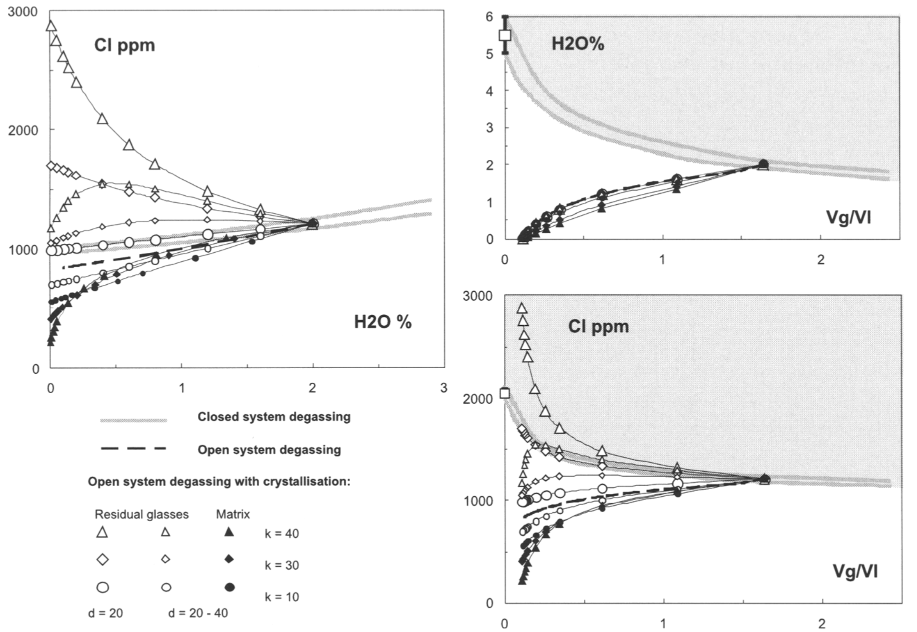

Fig. 2. Theoretical evolution of H_2O, Cl, and V_g/V_l in residual melts or groundmass (melt+microlites) for closed- and open-system degassing models: grey lines: closed-system evolution from initial melt (open square); initial melt compositions and d^{i}_{v-l} values correspond with those of the 650 years BP eruption at Mount Pelée (Table 1). Open-system degassing models are assumed to begin at $H_2O=2\%$, Cl=1100 ppm, and $V_g/V_l=1.7$. The discontinuous line indicates open-system degassing with no melt crystallization. Large open symbols indicate open-system degassing with degassing-induced crystallization ($k_{SV}=10$ to 40). Small open symbols indicate the same models, assuming an increase of the d^{Cl}_{v-l} values ($d=20$ to 40). Solid symbols indicate the same models calculated for the bulk groundmass (residual glass+microlites) compositions. Notice that in V_g/V_l-H_2O or -Cl diagrams, the stippled zone corresponds with the clasts having evolved in a closed system, including the possibility of gas expansion without further H_2O vapour exsolution (see Villemant & Boudon 1999). The lower half of the space (under closed-system evolution lines) corresponds with open-system degassing if no crystallization occurs. However, when degassing-induced crystallization occurs, and for large k_{SV} values, volatile halogen contents may sufficiently increase in residual melts, such that their compositions plot in the 'closed-system evolution domain'. Note, however, that such an effect is never encountered for H_2O.

open-system degassing model is not distinct from closed-system evolution.

On the contrary, when residual melt compositions are measured, very large variations in Cl contents are observed at high degrees of degassing. Halogen contents in residual melts, which may vary by one order of magnitude and may be much greater or lower than initial melt contents, are thus much more sensitive tracers of extreme degassing–crystallization steps than H_2O. Very large increases in halogen contents in residual melts are expected when crystallization rates are high relative to degassing rates (large k_{SV} values): the incompatible behaviour of halogens (enrichment in residual melts due to microlite crystallization) is not counterbalanced by their volatile behaviour (halogen extraction from the melt by the H_2O vapour phase). On the contrary, when the crystallization rate is low relative to the degassing rate, halogen extraction from the melt by the vapour phase dominates. Thus, the net result of these two opposite effects depends critically on the value of k_{SV}, which relates the degassing and the crystallization rates. For the chosen conditions (expected to act in a rhyolitic melt during a dome-building eruption), a net increase in the Cl content of the residual melt is observed when k_{SV} exceeds c.20. This value typically corresponds with the appearance of silica minerals at the liquidus of H_2O-saturated rhyolitic melts (Fig. 1). Finally, if possible variations of d^{Cl}_{v-l} values with the evolution of residual melt composition are taken into account, complex variations may be observed (see the fourth set of curves with d^{Cl}_{v-l} increasing from 20 to 40; Fig. 2).

Application to natural systems: the examples of Mount Pelée and Santa Maria-Santiaguito

Measurements of H_2O and Cl contents in glasses from dome-building eruptions are relatively abundant in the literature. However, because of the analytical difficulties mentioned above, numerous data-sets do not report halogen and H_2O measurements on the same glasses or melt inclusions. Published values for the Mount Pinatubo, Galeras, Mount St Helens and Soufrière Hills eruptions give some general information on the relative behaviour of H_2O and Cl during shallow degassing of rhyolitic melts during dome-building eruptions (Table 2). The main characteristics of all these eruptions are:

1. The H_2O contents of residual glasses in erupted products are generally significantly lower than estimated initial melt contents, as a result of magma degassing. The lowest measured H_2O contents are *c.* 0.5%, which generally corresponds with the analytical detection limits, and so lower H_2O contents in residual melts may thus be likely.
2. In the same glasses, Cl contents are much more highly variable than H_2O contents, and maximum values are similar to, or even higher than, those estimated in initial melts.
3. Composition ranges for Cl and H_2O are generally narrower in melt inclusions than in corresponding glasses, and the maximum values are close to estimated initial melt contents. It should be noted, however, that in most cases, initial melt content estimates are based on melt inclusion measurements, but these values are generally confirmed by experimental petrology. Such evolution of melt inclusion compositions probably reflects relatively deep degassing stages with simultaneous melt crystallization.

Water and halogen contents measured in both melt inclusions and residual melts thus provide consistent records of shallow magma degassing. The systematic variations of volatile abundances in volcanic products from different eruptions are qualitatively consistent with the degassing-crystallization models described above, which predict contrasting behaviours between H_2O and Cl.

Here we present H_2O and halogen measurements in both groundmass and residual melts of volcanic clasts from Plinian and dome-building eruptions of two volcanoes: Mount Pelée (Martinique, Lesser Antilles; Table 3) and Santa Maria (Guatemala; Table 4). Groundmass compositions were obtained from bulk-rock analyses, corrected for phenocryst contents as described in Villemant and Boudon (1999). Halogen (F, Cl, and Br) compositions of bulk rocks were measured using pyrohydrolysis and ion chromatography (F, Cl) or ICP–MS (Br) (Michel & Villemant, submitted); crystallinities were measured by both SEM image analysis and mass-balance calculations (Villemant & Boudon 1998). Bulk-rock H_2O contents were measured by H_2 manometry. Mean 2σ errors estimated by reproducibility on repeated analyses (and including errors on crystallinity measurements) are *c.* 10% for H_2O, Cl, and Br. Spot analyses of H_2O and Cl in glasses (residual melts and melt inclusions) were performed using electron-probe (CAMECA, 15 kV, 5 nA), scanning analysis. Water contents were calculated using the 'difference to 100%' method. Each value represents a mean of three to five individual measurements on the same glassy area (100–200 μm across). Mean errors are *c.* 15–20% for both H_2O and Cl.

Table 2. *Ranges of H_2O and Cl contents measured in glasses and melt inclusions of different eruptions.*

	Initial contents estimates*		Melt inclusions		Glasses	
	H_2O (%)	Cl (ppm)	H_2O (%)	Cl (ppm)	H_2O (%)	Cl (ppm)
Pinatubo	6	1250	5.5–6.4	1250–880	2.5–0.30	1500–400
Soufrière Hills	4–5	3400	6.6–2	4400–1000	3.6–1.9	3200–10
Mount St Helens	5		7.5?–2.5		3.5–0.45	
Galeras	?	?	2.4–0.3	2700–700	1–0.6	1200–400
Mount Pelée	5.5	2100	6–1.3	2300–1000	2.8–0.1	1700–25

*Estimates from melt inclusion analysis and/or experiments.
References: Pinatubo: Gerlach *et al.* (1996); Rutherford and Devine (1996); Soufrière Hills: Devine *et al.* (1998); Edmonds *et al.* (2001); Mount St Helens: Melson (1983); Rutherford *et al.* (1985); Galeras: Stix *et al.* (1997); Mount Pelée: Martel *et al.* (1998); Villemant and Boudon (1999).

Table 3. *Composition of residual glasses in clasts from the 650 years* BP *eruption (Mount Pelée).*

	1310K1		ML 801-b		MB 1101				MF 1001A					
H_2O (%)	1.85	3.91	1.22	0.38	3.13	1.02	<0.05	1.02	<0.05	2.81	3.44	0.77	0.39	1.08
Cl (ppm)	1080	1625	1903	1887	1627	1890	1619	1910	1328	1348	1906	2056	1315	1860

Measurements by electron probe (CAMECA, 15 kV, 5 nA, scanning analysis). Water is calculated using the 'difference to 100%' method. Each value represent a mean of three to five individual measurements on a same glassy area (100–200 μm). Mean errors are *c.* 15–20 % for both H_2O and Cl.

Table 4. *Composition of groundmass and residual glasses in clasts from the Plinian- and dome-building eruptions of Santa Maria volcano (Guatemala).*

Dome clasts and lava domes and flows (1929 to present day – Santiaguito)

	C3-1	C3-3	C3-7	SM-8	13	12	10a	10b	11	15
H_2O (%)	0.93	0.36	0.35	0.62	0.38	0.23	0.22	0.07	0.39	0.70
Cl (ppm)	651	344	114	573	396	466	397	343	385	676
Br (ppm)	1.92	1.01	2.14	1.61	1.47	1.41	1.12	1.14	1.48	1.65

Plinian fall (1902 eruption)

	B2-1	C2-1	C2-12	D2-4	D2-8	E2-1	E2-2	E2-9	6-C2a	6-C2b	6-B2a	6-B2b	14	6-E0
H_2O (%)	1.33	1.38	1.32	1.21	1.09	1.04	1.10	1.27	0.55	2.12	1.82	1.00	1.53	7.01
Cl (ppm)	934	1238	780	842	809	875	886	834	937	1258	1397	1195	922	1380
Br (ppm)	1.26	2.07	1.63	2.39	1.24	1.84	1.94	1.75	–	–	–	–	1.89	–

Glasses – Plinian fall (1902 eruption)

	SM6-C2					SM6-B2				
H_2O (%)	0.55	2.12	2.37	2.37	0.80	2.07	1.25	1.25	1.82	1.00
Cl (ppm)	937	1258	1390	1125	937	1397	1155	1235	1397	1195

Groundmass compositions (H_2O, Cl and Br) are calculated from bulk-rock analyses, and the compositions of residual glasses (H_2O, Cl) are measured by electron probe (see Table 3 and text).

Representative major-element compositions of initial melts estimated from melt inclusions measurements are also reported in Table 5.

The 650 years BP eruption at Mount Pelée (Pl eruption) was a complex eruption with a succession of dome-building (Peléean) eruptions and a Plinian eruption in a short interval of time (Villemant *et al.* 1996; Villemant & Boudon 1998). The different evolution paths evidenced by the variation in volatile contents (H_2O, F, Cl, and Br) measured in bulk clasts have been interpreted in terms of closed- and open-system degassing models (Villemant & Boudon 1999). New Cl and H_2O measurements on residual glasses by electron-probe analysis are reported in Table 3. Bulk-rock analyses corrected for phenocryst contents and residual glass analyses are represented in Cl–H_2O–V_g/V_l diagrams (Fig. 3).

Table 5. *Representative major-element compositions of initial melts: measurements on melt inclusions.*

	1310K1	SM6
SiO_2	74.49	72.9
TiO_2	0.32	0.30
Al_2O_3	13.82	14.6
Fe_2O_3	2.58	2.50
MnO	0.09	0.20
MgO	0.42	0.50
CaO	2.60	1.80
Na_2O	3.69	4.90
K_2O	1.99	2.30
Total	100.00	100.0

1310K1: 650 years BP eruption at Mount Pelée, SM6: 1902 Plinian eruption at Santa Maria (from Villemant & Boudon 1999, and Poteaux 1998, unpublished).

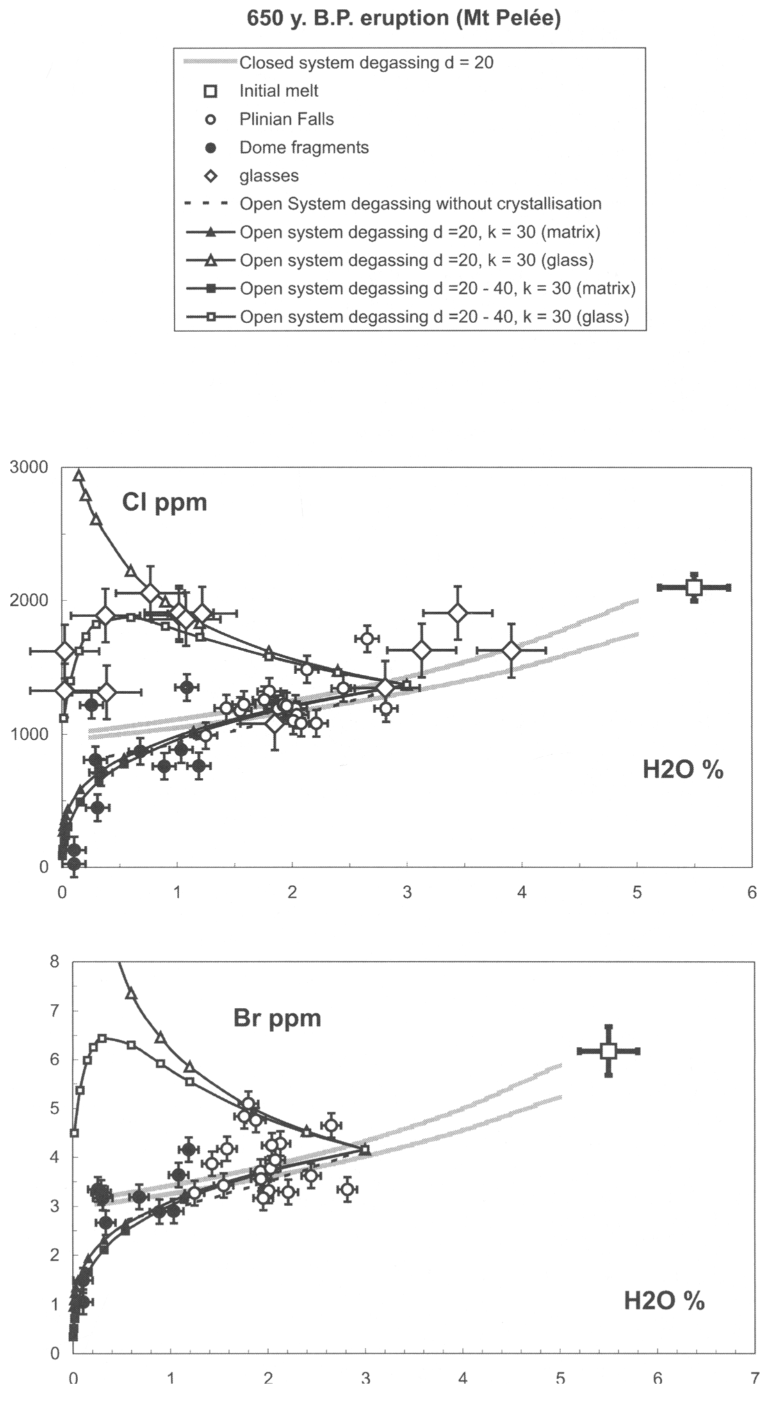

Fig. 3. Matrix and glass analyses of volcanic clasts from the 650 years BP eruption at Mount Pelée, Martinique: closed circles indicate dome clasts (groundmass compositions); open circles indicate Plinian clasts (groundmass compositions); open diamonds represent glass compositions in Plinian- or dome- clasts. Open squares indicate the initial melt composition (from Villemant & Boudon 1998). Evolution lines are the same as in Figure 2. Grey lines

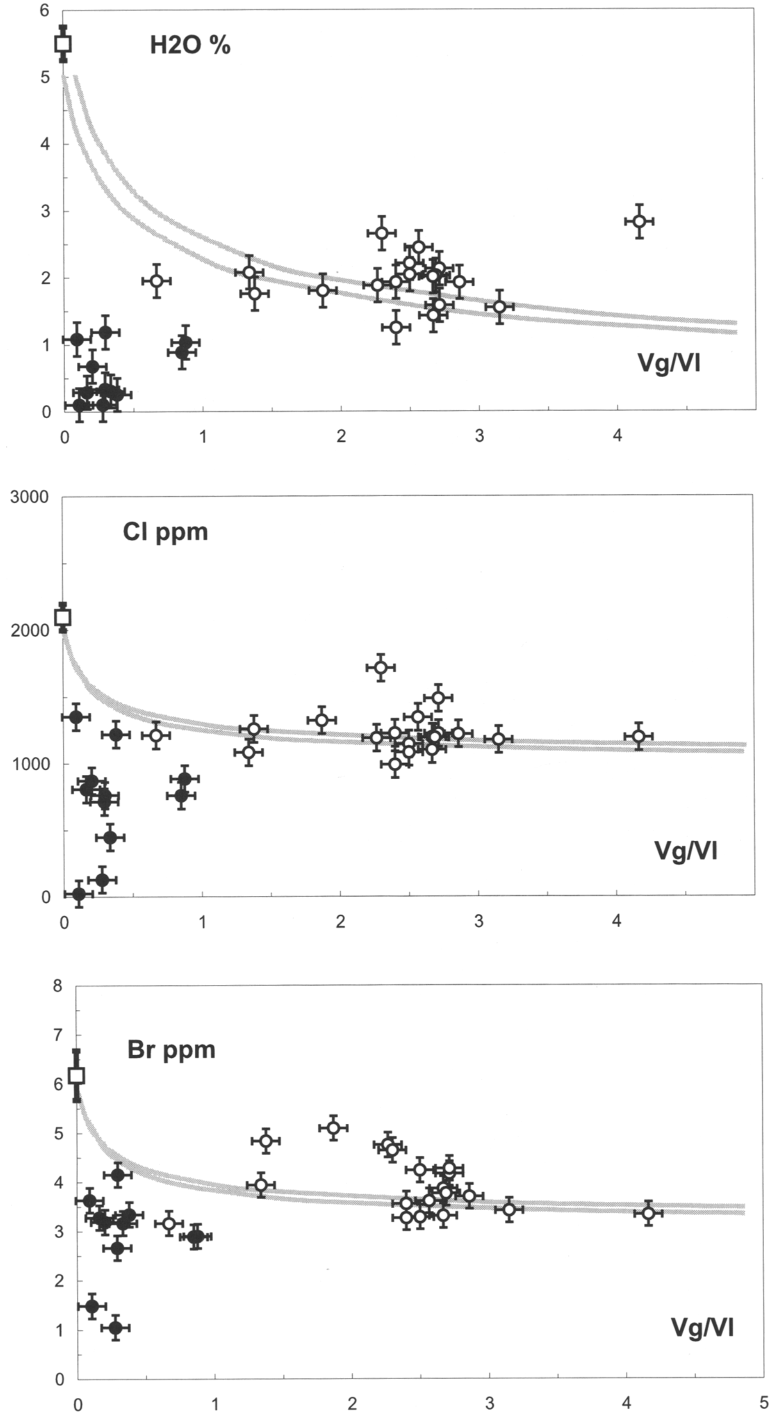

indicate closed-system evolution. Solid lines indicate open-system evolution; solid symbols represent groundmass compositions (data from Villemant & Boudon 1999); open symbols indicate residual melt compositions (see Table 3). Open-system evolution is arbitrarily calculated from initial compositions on the closed-system evolution lines (H_2O=3%); (1) $k_{SV}=30$, $d^{Cl}_{v-l}=20$; $d^{Br}_{v-l}=18$ and (2) $k_{SV}=30$, $d^{Cl}_{v-l}=20-40$; $d^{Br}_{v-l}=18-36$.

The 1902 Plinian eruption and the 1922–present-day dome-building eruption of Santa Maria volcano

The recent activity of the Santa Maria volcano started in 1902 with a climactic Plinian eruption (Rose 1972; Williams & Self 1983). In 1922, the construction of successive lava domes and thick lava flows (called Santiaguito) began in the caldera resulting from the 1902 eruption. Continuing activity up to the present has produced numerous dome collapse events (Rose 1973). Water and halogen measurements of groundmass and residual melts in clasts from the 1902 Plinian eruption, the 1929 block-and-ash flows and in different lava flows and lava domes of the 1947–present-day period of activity, are reported in Table 4 and represented in Figure 4.

Correlation diagrams between V_g/V_l and H_2O or halogen (Cl, Br) contents of groundmasses for both series clearly show that most Plinian clasts correspond with closed-system evolution, which can be simply deduced from the initial melt compositions and equations 1 to 3. In contrast to this, dome clast compositions typically correspond with open-system degassing with gas loss,

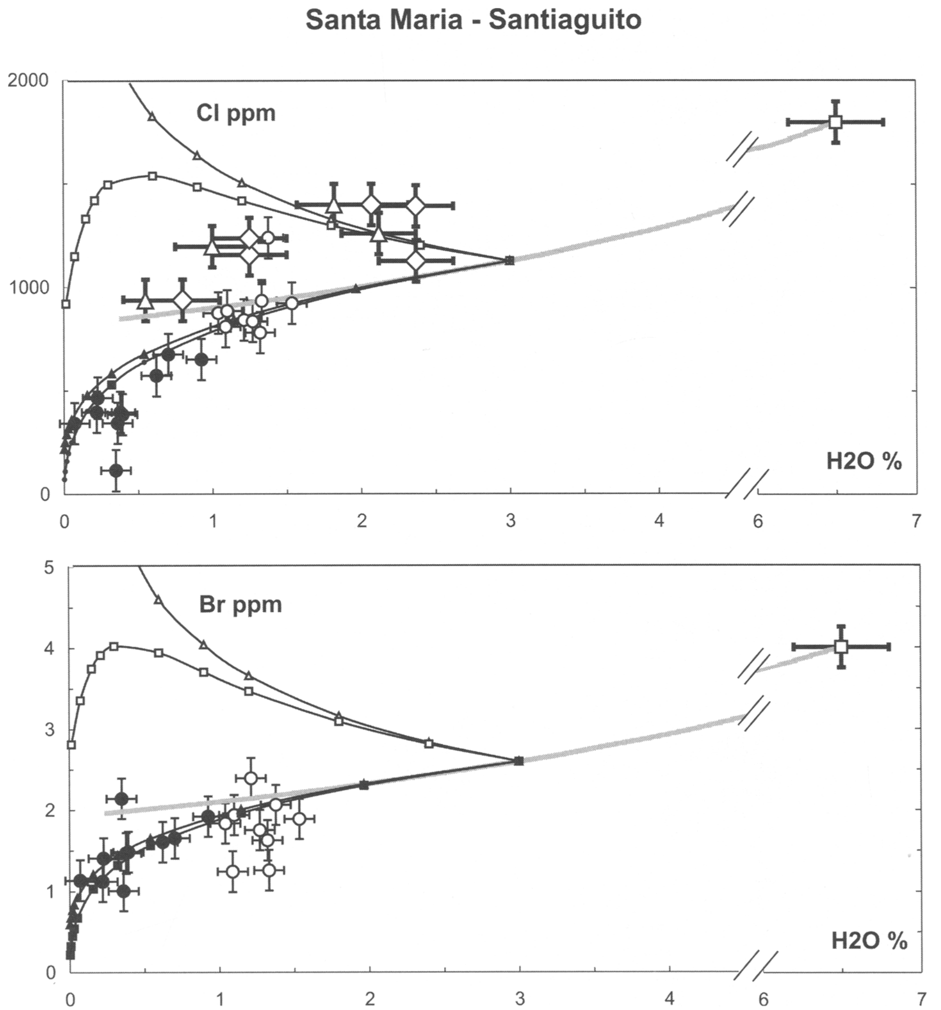

Fig. 4. Matrix and glass analyses of volcanic clasts from the Santa Maria-Santiaguito eruptions (1902–present day, Guatemala). Symbols and evolution lines as in Figure 3. Closed circles indicate dome clasts or lava flows (1922–present-day activity), groundmass compositions; open circles represent Plinian clasts (1902 eruption),

evidenced by a large decrease of the V_g/V_l values with decreasing volatile content. As stated above, however, it is not possible to identify more precisely the conditions of these open-system degassing processes in the absence of an independent measurement of the ratio between exsolved and lost vapour.

More complete information is obtained when spot analyses of residual glasses are used. The available analytical techniques only provide information on the H_2O and Cl contents of residual melts. Water–Cl correlation diagrams for both volcanic series clearly show that the effects of degassing-related crystallization are significant on halogen behaviour. Chlorine enrichment in residual melts is significant, and may be as high as in initial melts as exemplified by clasts of the 650 years BP eruption of Mount Pelée (Fig. 3). Such an enrichment may be modelled using a high k_{SV} value, which corresponds with highly evolved melts, eventually corresponding with crystallization of silica minerals. For the 650 years BP eruption of Mount Pelée, this is consistent with SEM and TEM observations of dome clasts, which show that residual glasses are highly microcrystalline with abundant plagioclase

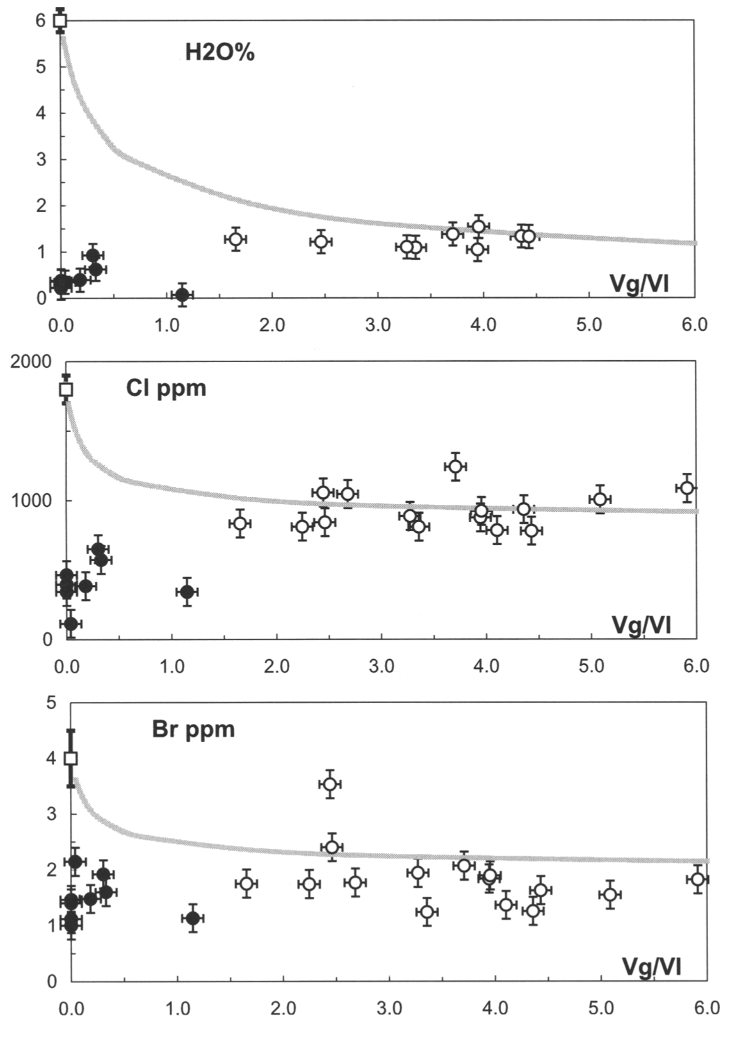

groundmass compositions (Table 4); open squares indicate initial melt compositions estimated from melt inclusions (S. Poteaux, unpublished data).

microlites and the presence of quartz nanolites (Villemant *et al.* 1996; Villemant & Boudon 1998; Nougrigat *et al* in prep.).

If the measured glass compositions represent different steps of the same continuous degassing process, H_2O–Cl diagrams show that crystallization–degassing processes do not occur at constant $d^{Cl}_{v\text{-}l}$ and/or k_{SV}. The complex variations of the residual melt compositions may be explained by large k_{SV} values and a significant increase in $d^{Cl}_{v\text{-}l}$ values, both related to melt differentiation due to degassing-induced crystallization at shallow depth.

Models of degassing processes at shallow depths are well constrained by the H_2O and halogen contents of residual melts. A combination of both bulk-rock analyses (corrected from phenocryst contents), and spot analyses of glasses and of micro-textural characteristics of erupted clasts (dome or Plinian clasts) allow identification of the relative importance of H_2O degassing and crystallization processes in H_2O-rich rhyolitic melts during their transfer to the surface by volcanic eruptions. The study of well-documented Plinian and dome-building eruptions (the 1902 to present-day eruptions at Santa Maria-Santiaguito volcano, Guatemala, and the 650 years BP eruption at Mount Pelée, Martinique) show that Plinian and dome-building eruptions display distinct signatures for H_2O, halogens (Cl, Br) and vesicularities. In particular, spot analyses of glasses show that during the slow degassing processes characterizing dome-building eruptions, degassing-induced crystallization leads to large variations in halogen contents. These variations are the result of two opposing effects: (1) melt crystallization, which induces an increase of halogens in the residual melt due to their incompatible character, and (2) halogen extraction by the vapour phase. This latter effect depends on the relative mass fractions of crystallizing microlites and exsolving vapour and on the variation in halogen partition coefficients between vapour and melt; both depend on the major-element composition of the residual melt, which may be modelled using experimental data or thermodynamic codes. The main difficulty of these modelling methods involves the determination of halogen partition coefficients and their dependence on P, T, and melt compositions and on possible kinetic effects. In this study, we show that in order to interpret the variations of Cl contents in residual melts of dome-building eruptions, large variations of $d^{Cl}_{v\text{-}l}$ values during the last stages of crystallization–degassing process must be assumed, which is consistent with some experimental results. On the contrary, such large variations in Cl contents – observed in the residual melts of Soufrière Hills volcano (Montserrat) are considered as incompatible with crystallization–degassing processes alone and, on the basis of hydrogen isotope measurements, have been interpreted as the result of dome leaching by groundwater circulation (Harford 2000). Such divergent interpretations show that, in addition to the fact that both syn-eruptive and late-eruptive processes may affect the volatile contents of residual melts of dome magmas, there is a great need for further experimental work to improve constraints on halogen behaviour during shallow-depth magma degassing.

This modelling shows that the halogen content of the residual melts, and consequently of the exsolved vapour phases, directly depends on the kinetics of melt degassing and magma ascent rate and, for dome-building eruptions, on the extent of melt crystallization–degassing process. Fluid compositions calculated from theoretical residual melt compositions and d values show that, with an increasing fraction of extracted H_2O vapour, Plinian eruptions (closed-system) produce Cl-poor vapour, while dome-building eruptions (open-system degassing with crystallization) are much more efficient at extracting volatile halogens (Cl, Br, and probably I), leading to HCl-, HBr- and HI-rich vapours (Fig. 5). Since F is very weakly extracted into vapour phase ($d^{F}_{v\text{-}l} < 1$), volcanic gases are relatively HF-poor, and the F concentration in the melt should be constant when there is no melt crystallization and should increase with advancing degassing-induced crystallization, because of the incompatible character of halogens. Measurements of HF and HCl contents of volcanic gases thus should provide precise indications of the degassing regime at shallow depth: for example, the above models suggest that volcanic gases should have increasing HCl/HF and decreasing HCl contents when the eruptive style evolves from effusive to explosive. In addition, these models predict that during dome-building eruptions the HCl/HF ratio of gases should vary with the different phases of eruptive activity. However, HCl emission rates and HCl/HF or HCl/SO_2 ratios measured in volcanic plumes by spectroscopic techniques (see e.g. Edmonds *et al.* 2002) display highly variable situations, which indicate that many processes other than those described by the above models at the scale of the residual melts in erupted magma fragments, determine the final composition of the gases expelled by the volcanic vents. In particular, large variations in the degassing conditions, such as the ratio between

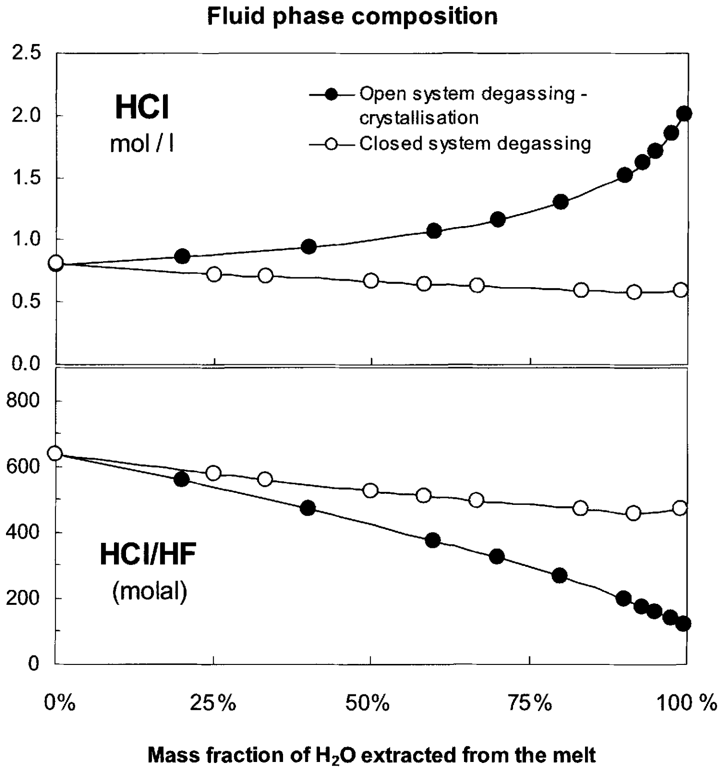

Fig. 5. Theoretical evolution of HCl and HF/HCl ratios of volcanic gases during closed- and open-system degassing.Gas compositions are calculated from residual melt compositions using d^{i}_{v-l} values (d^{Cl}_{v-l}=20 and d^{F}_{v-l}=0.1). The initial melt composition (H_2O=3%) and the degassing paths are the same as in Figures 3 and 4 (closed- and open-system degassing). The HCl content and HCl/HF ratio of volcanic gases vary with the eruptive style and the progress of the degassing process.

gas escape and degassing-induced crystallization, are expected to occur over the whole magma body, and are ultimately reflected in the gas composition of the volcanic plume. The relative importance of these different contributions is especially dependent on the variations of conduit geometry and permeability, the magma extrusion and ascent rates, etc. Thus, interpretation of juvenile volcanic gas compositions must integrate various chemical and physical processes acting at different scales, which requires multidisciplinary approaches, among which analytical and experimental petrology and chemistry play a critical role.

J. C. Komorowski, C. Oppenheimer, D. Pyle and an unknown reviewer are thanked for their comments and fruitful discussions. This research was supported by the PNRN programme (CNRS, France) and the Central America Research Programmes of the French Foreign Office.

References

Blundy, J. & Cashman K.V. 2001. Ascent-driven crystallisation of dacite magmas at Mount St Helens, 1980–1986. *Contributions to Mineralogy and Petrology*, **140**, 631–650.

Bourdier, J. L., Boudon, G. & Gourgaud, A. 1989. Stratigraphy of the 1902 & 1929 nuée ardente deposits, Mt Pelée, Martinique. *In*: Boudon, G. & Gourgaud, A. (eds) Mount Pelée. *Journal of Volcanology and Geothermal Research*, **38**, 77–96.

Burnham, C.W. 1979. The importance of volatile constituents. *In: The Evolution of Igneous Rocks: Fiftieth Anniversary Perspectives*. Princeton: Princeton University Press, 439–482.

Burnham, C.W. 1994. Development of the Burnham model for prediction of H_2O solubility in magmas. *In*: Carroll, M. & Holloway, J.R. (eds) *Volatiles in Magmas*. Reviews in Mineralogy, **30**, 123–129, Mineralogical Society of America, Washington D.C.

Bureau, H., Keppler, H. & Métrich, N. 2000. Volcanic degassing of bromine and iodine: experimental fluid/melt partitioning data and application to stratospheric chemistry. *Earth and Planetary Science Letters*, **183**, 51–55.

BURSIK, M. 1993. Subplinian eruption mechanisms inferred from volatile and clast dispersal data. *Journal of Volcanology and Geothermal Research*, **57**, 57–70.

CASHMAN, K.V. 1992. Groundmass crystallisation of Mount St Helens dacite, 1980–1986: a tool for interpreting shallow magmatic processes. *Contributions to Mineralogy and Petrology*, **109**, 441–449.

CASHMAN, K. V. & BLUNDY, J. 2000. Degassing and crystallisation of ascending andesite and dacite. *Philosophical Transactions of the Royal Society of London*, A**358**, 1487–1513.

DEVINE, J. D., MURPHY, M. D., RUTHERFORD, M. J., BARCLAY, J., SPARKS, R. S. J., CARROLL, M. R., YOUNG, S. R. & GARDNER, J. E. 1998. Petrologic evidence for pre-eruptive pressure–temperature conditions, and recent reheating, of andesitic magma erupting at the Soufrière Hills volcano, Montserrat, W.I. *Geophysical Research Letters*, **19**, 3669–3672.

EDMONDS, M., PYLE, D. & OPPENHEIMER, C. 2001. A model for degassing at the Soufrière Hills Volcano, Montserrat, West Indies, based on geochemical data. *Earth and Planetary Science Letters*, **186**, 159–173.

EDMONDS, M., PYLE, D. & OPPENHEIMER, C. 2002. HCl emission at Soufrière Hills Volcano, Montserrat, West Indies, during a second phase of dome building: November 1999 to October 2000. *Bulletin of Volcanology* **64**, 21-30.

EICHELBERGER, J. C. 1995. Silicic volcanism: ascent of viscous magmas from crustal reservoirs. *Annual Review of Earth and Planetary Science Letters*, **23**, 41–63.

EICHELBERGER, J. C., CARRIGAN, C. R., WESTRICH, H. R. & PRICE, R. H. 1986. Non-explosive silicic volcanism. *Nature*, **323**, 598–602.

GARDNER, J. E., THOMAS, R. M. E., JAUPART, C. & TAIT, S. 1996. Fragmentation of magma during Plinian volcanic eruptions. *Bulletin of Volcanology*, **58**, 144–162.

GARDNER, J. E., RUTHERFORD, M. & HORT, M. 1998. Degassing of trace gases during volcanic eruptions. *EOS, Transactions of the American Geophysical Union*, **79**, F936.

GERLACH, T. M., WESTRICH, H. R. & SYMONDS, R. 1996. Preeuption vapour in magma of the climactic Mount Pinatubo eruption: source of the giant stratospheric sulfur dioxide cloud. *In:* NEWHALL, C. & PUNONGBAYAN, R. (eds) *Fire and Mud: Eruptions and Lahars of Mount Pinatubo, Philippines.* University of Washington Press, Seattle, 415–433.

GHIORSO, M. S. & SACK, R. O. 1995. Chemical mass transfer in magmatic processes IV. A revised and internally consistent thermodynamic model for the interpolation and extrapolation of liquid–solid equilibria in magmatic systems at elevated temperatures and pressures. *Contributions to Mineralogy and Petrology*, **119**, 197–212.

HAMMER, J. E., CASHMAN, K.V., HOBLITT, R. P. & NEWMAN, S. 1999. Degassing and microlite crystallisation during the pre-climactic events of the 1991 eruption of the Mt Pinatubo, Philippines. *Bulletin of Volcanology*, **60**, 355–380.

IHINGER, P. D., HERVIG, R. L. & MCMILLAN, P. F. 1994. Analytical methods for volatiles in glasses. *In:* CARROLL, M. R. & HOLLOWAY, J. R. (eds) *Volatiles in Magmas*. Reviews in Mineralogy, **30**, 66–121, Mineralogical Society of America, Washington D.C.

HARFORD, C. 2000. *The Volcanic Evolution of Montserrat*. PhD Thesis, University of Bristol, 195 pp.

JAUPART, C. & ALLÈGRE, C. J. 1991. Gas content, eruption rate and instabilities in silicic volcanoes. *Earth and Planetary Science Letters*, **102**, 413–429.

KILINC, I. A. & BURNHAM, C. W. 1972. Partitioning of chloride between silicate melts and coexisting aqueous phase from 2 to 8 kbars. *Economic Geology*, **67**, 231–235.

KRAVCHUK, I. F. & KEPPLER, H. 1994. Distribution of chloride between aqueous fluids and felsic melts at 2 kbar and 800°C. *European Journal of Mineralogy*, **6**, 913–923.

LEJEUNE, A.-M. & RICHET, P. 1995. Rheology of crystal bearing silicate melts: an experimental study at high viscosities. *Journal of Geophysical Research*, **100**, 4215–4229.

MARTEL, C., PICHAVANT, M., BOURDIER, J. L., TRAINEAU, H., HOLTZ, F. & SCAILLET, B. 1998. Magma storage and control of eruption regime in silicic volcanoes: experimental evidence from Mt. Pelée. *Earth and Planetary Science Letters*, **156**, 89–99.

MELNIK, O. & SPARKS, R. S. J. 1999. Nonlinear dynamics of lava dome extrusion. *Nature*, **402**, 37–41.

MELSON, W.G. 1983. Monitoring the 1980–1982 eruptions of Mount St. Helens: compositions and abundances of glass. *Science*, **221**, 1387–1391.

MÉTRICH, N. & RUTHERFORD, M. J. 1992. Experimental study of chlorine behaviour in hydrous silicic melts. *Geochimica et Cosmochimica Acta*, **56**, 607–616.

MICHEL, A. & VILLEMANT, B. Determination of halogens (F, Cl, Br, I), sulphur and water in 17 reference geological material. *Geostandard Newsletter* (submitted).

NOUGRIGAT, S., VILLEMANT, B., BOUDON, G., BESSON, P. & KOMOROWSKI, J.C. (in preparation). Origin of lava dome explosivity: the 1902 and 1929 eruptions of Montagne Pelée (Martinique, Lesser Antilles).

ROBERTSON, R., COLE, P., SPARKS, R. S. J., HARFORD, C., LEJEUNE, A. M., MCGUIRE, W. J., MILLER, A. D., MURPHY, M. D., NORTON, G., STEVENS, N. F. & YOUNG, S. R.1998. The explosive eruption of Soufrière Hills Volcano, Montserrat, West Indies, 17 September 1996. *Geophysical Research Letters*, **25(18)**, 3429–3432.

ROSE, W. I. 1973. Notes on the 1902 eruption of Santa Maria volcano, Guatemala. *Bulletin of Volcanology*, **36**, 29–45.

RUTHERFORD, M. J. & DEVINE, J. D. 1996. Preeruption pressure temperature conditions and volatiles in the 1991 dacitic magma of Mount Pinatubo. *In:*

NEWHALL, C. & PUNONGBAYAN, R. (eds) *Fire and Mud: Eruptions and Lahars of Mount Pinatubo, Philippines*. University of Washington Press, Seattle, 751–766.

RUTHERFORD, M. J., SIGURDSSON, H., CAREY, S. & DAVIS, A. 1985. The May 18, 1980, eruption of Mount St. Helens. 1. Melt composition and experimental phase equilibria. *Journal of Geophysical Research*, **90**, 2929–2947.

SCHNETGER, B., MURAMATSU, Y. & YOSHIDA, S. 1998. Iodine (and other halogens) in twenty six geological reference materials by ICP–MS and ion chromatography. *Geostandards Newsletter,* **22**, 181–186.

SHINOHARA, H., IIYAMA, J. T. & MATSUO, S. 1989. Partition of chlorine compounds between silicate melt and hydrothermal solutions: I partition of NaCl–KCl. *Geochimica et Cosmochimica Acta*, **53**, 2617–2630.

SIGNORELLI, S. & CARROLL, M. R. 2000. Solubility and fluid-melt partitioning of Cl in hydrous phonolitic melts. *Geochimica et Cosmochimica Acta*, **64**, 2851–2862.

SIGNORELLI, S. & CARROLL, M. R. 2001. Experimental constraints on the origin of chlorine emissions at the Soufrière Hills volcano, Montserrat. *Bulletin of Volcanology*, **62,** 431–440.

SPARKS, R. S. J. 1997. Causes and consequences of pressurisation in lava dome eruptions. *Earth and Planetary Science Letters*, **150**, 177–189.

SPARKS, R. S. J. 2003. Dynamics of magma degassing. *In:* OPPENHEIMER, C., PYLE, D. M. & BARCLAY, J. (eds) *Volcanic Degassing*, Geological Society of London, Special Publications, **213,** 5–22.

STIX, J., TORRES, R. C., NARVAEZ, L. M., CORTÉS, G. P. J., RAIGOSA, J. A., GOMEZ, D. M. & CASTONGUAY, R. 1997. A model for vulcanian eruption at Galeras volcano, Colombia. *Journal of Volcanology and Geothermal Research*, **77**, 285–303.

SWANSON, S. E., NANEY, M. T., WESTRICH, H. R. & EICHELBERGER, J. C. 1989. Crystallisation history of Obsidian dome, Inyo Domes, California. *Bulletin of Volcanology*, **51**, 161–176.

SYMONDS, R.B., ROSE, W.I., BLUTH, G.J.S. & GERLACH, T.M. 1994. Volcanic gas studies: methods, results and applications. *In*: CARROL, M.R. & HOLLOWAY, J.R. (eds) *Volatiles in magmas.* Min. Soc. of Am., Washington DC Reviews in Mineralogy, **30**, 66–121.

TUTTLE, O. F. & BOWEN, N. L. 1958. *Origin of Granite in the Light of Experimental Studies in the System* $NaAlASi_3O_8$*–*$KAlSi_3O_8$*–*SiO_2*–*H_2O*.* Geological Society of America, Memoir, **74**, 153.

VILLEMANT, B. & BOUDON, G. 1998. Transition between dome-building and plinian eruptive styles: H_2O and Cl degassing behaviour. *Nature*, **392**, 65–69.

VILLEMANT, B. & BOUDON, G. 1999. H_2O and halogen (F, Cl, Br) behaviour during shallow magma degassing processes. *Earth and Planetary Science Letters*, **168**, 271–286.

VILLEMANT, B., BOUDON, G. & KOMOROWSKI, J. C. 1996. U-series disequilibrium in arc magmas induced by water–magma interaction. *Earth and Planetary Science Lett*ers, **140**, 259–267.

WEBSTER, J. D. 1992. Water solubility and chlorine partitioning in Cl-rich granitic systems: effects of melt composition at 2 kbar and 800°C. *Geochimica et Cosmochimica Acta,* **56**, 679–687.

WEBSTER, J. D. & HOLLOWAY, J. R. 1988. Experimental constraints on the partitioning of Cl between topaz rhyolite melt and H_2O and H_2O+CO_2 fluids: new implications for granitic differentiation and ore deposition. *Geochimica et Cosmochimica Acta*, **52,** 2091–2105.

WEBSTER, J. D., KINZLER, R. J. & MATHEZ, E. A. 1999. Chloride and water solubility in basalt and andesite melts and implications for magmatic degassing. *Geochimica et Cosmochimica Acta*, **63**, 729–738.

WILLIAMS, S. N. & SELF, S. 1983. The October 1902 plinian eruption of Santa Maria volcano, Guatemala. *Journal of Volcanology and Geothermal Research*, **16**, 33–56.

WILSON, L., SPARKS, S. & WALKER, G. 1980. Explosive volcanic eruptions IV: the control of magma properties and conduit geometry on eruption column behaviour. *Geophysical Journal of the Royal Astronomical Society*, **63**, 117–148.